

Numerical simulation of interface deformation and wave resistance caused by a given pressure load moving in an ice-breaking channel

B.-Y. Ni*, L.-D. Zeng

College of Shipbuilding Engineering, Harbin Engineering University, Harbin, China, 150001

* corresponding author, e-mail: nibaoyu@hrbeu.edu.cn

1. Introduction

It has been observed that Air Cushion Vehicle (ACV) could be used to rupture ice by taking advantage of the fact that moving load can generate waves in both ice and water. There has been many studies carried out in moving loads on ice sheet from analytical solution, numerical simulation and experimental study [1]. It has been found that the response of ice under the moving load depends on the velocity of the load. When the velocity of the load is less than the minimum phase speed c_{\min} predicted by the linear dispersion relation, the disturbance is localized and waves do not propagate away from the load. If the velocity of the load approaches c_{\min} , the amplitude of the waves increases and some oscillations start to appear around the load. Otherwise, for the velocities greater than c_{\min} , waves of different wavelengths appear before and after the load [1]. It seems that there has been little work which considers the response of the moving loads in an ice-breaking channel, or the ice-water-ice domain. Along with the development of the arctic route, this problem becomes more practical and the interface deformation and wave transformation in this kind of domain arouse the interest of this study. Based on the desingularized Rankine panel method developed by [2], this work extends to calculate the interface deformation and wave resistance of the moving loads in an ice-breaking channel and compares these results with those on the ice sheet, which have been validated by the theoretical solutions.

2. Mathematical formulation

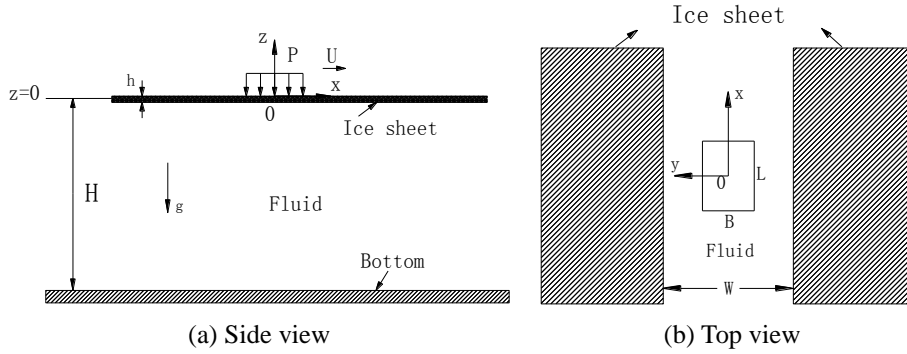


Fig.1 Sketch of the problem

Fig.1 gives a sketch of the problem, which shows a given pressure load with length L and breadth B moving in an ice-breaking channel at a constant speed U . The ice-breaking channel is W wide and the ice sheets on two sides are assumed to be infinite, homogeneous and unbroken ice with thickness h and density $\rho_i = 900 \text{ kg/m}^3$. Moreover, the water body is taken to be of constant density $\rho_w = 1000 \text{ kg/m}^3$ and uniform depth H . We establish a coordinate system that moves with the load in the positive direction of the x -axis and set the origin O at the center of the load and z -axis pointing upwards, opposite to the gravitational acceleration g .

In this moving coordinate system, the flow becomes steady. We assume the fluid is inviscid and incompressible, and the flow beneath the ice sheet is irrotational. Thus, a velocity potential ϕ can be introduced, which is composed of flow velocity potential $-Ux$ and disturbance potential $\phi(x, y, z)$. In the fluid domain, the disturbance potential satisfies Laplace's equation

$$\frac{\partial^2 \phi}{\partial x^2} + \frac{\partial^2 \phi}{\partial y^2} + \frac{\partial^2 \phi}{\partial z^2} = 0 \quad (1)$$

Ice sheet can be treated as an isotropic, homogeneous, viscoelastic thin plate of uniform thickness. This material can be described using Kelvin-Voigt model [3]. If $\eta(x, y)$ represents a small vertical ice-sheet deflection, then the linearized boundary conditions (BC) of the moving load in an ice-breaking channel can be described as

$$\left\{ \begin{array}{l} \frac{Gh^3}{3}(1-\tau U \frac{\partial}{\partial x})\nabla^4 \eta + \rho_i h U^2 \frac{\partial^2 \eta}{\partial x^2} = -\rho_w(-U \frac{\partial \varphi}{\partial x} + g\eta) \quad (|y| \geq W/2, z=0) \\ \rho_w g \eta - \rho_w U \frac{\partial \varphi}{\partial x} = -P(x, y) \quad (|y| < W/2, z=0) \\ \frac{\partial \varphi}{\partial z} = -U \frac{\partial \eta}{\partial x} \quad (z=0) \\ \frac{\partial \varphi}{\partial z} = 0, \eta = 0 \quad (z=-H) \\ \nabla \varphi = 0, \eta = 0 \quad (|x| \rightarrow \infty, z=0) \end{array} \right. \quad \begin{array}{l} (2a) \\ (2b) \\ (2c) \\ (2d) \\ (2e) \end{array}$$

where $G = 0.5E/(1 + \mu)$ is the shear elastic modulus of the ice with E as Young's modulus and $\mu = 1/3$ as Poisson's ratio for ice, τ is the relaxation time of ice sheet. $P(x, y)$ is the external pressure, which will be given below. At $|y| = W/2$, we neglect the influence caused by ice thickness, which causes an abrupt change of boundary condition there.

Combining Eq. (2a), Eq. (2c) and Eq. (2e), we obtain combined BC on ice

$$\frac{Gh^3}{3\rho_w g} \nabla^4 \int_x^{+\infty} \frac{\partial \varphi}{\partial z} dx + \frac{Gh^3 U \tau}{3\rho_w g} \nabla^4 \frac{\partial \varphi}{\partial z} + \int_x^{+\infty} \frac{\partial \varphi}{\partial z} dx - \frac{U^2}{g} \frac{\partial^2 \varphi}{\partial x^2} - \frac{\rho_i h U^2}{\rho_w g} \frac{\partial^2 \varphi}{\partial x \partial z} = -\frac{U}{\rho_w g} P \quad (3)$$

when h is taken as 0, Eq. (3) degenerates to the combined BC on water.

The moving pressure $P(x, y)$ is given in the form

$$P(x, y) = \frac{P_0}{4} \left\{ \tanh \left[\alpha \left(x - \frac{L}{2} \right) \right] - \tanh \left[\alpha \left(x + \frac{L}{2} \right) \right] \right\} \cdot \left\{ \tanh \left[\beta \left(y - \frac{B}{2} \right) \right] - \tanh \left[\beta \left(y + \frac{B}{2} \right) \right] \right\} \quad (4)$$

where P_0 is the nominal pressure, α and β are the parameters which control the rate of pressure fall-off at the edges, and $\alpha = \beta = 0.5$ in this paper. We take $P = 0$ outside the moving load area.

The free surface S_F discretization involves regular grids with $n+1$ points in the x -direction, approximating $(-\infty, +\infty)$, and $m+1$ points in the y -direction, approximating $(-\infty, +\infty)$. In this paper, the free surface is truncated at $(-7L, 3L)$ and $(-5L, 5L)$ in x - and y -directions, respectively. The uniform mesh sizes on the x - and y -axes are denoted by Δx and Δy . Then we put the source panels at a distance Δx above the free surface to avoid the singularity. The collection points are located at the panel centers on the free surface. Introducing the Green function $1/r$, we obtain

$$\varphi(x, y, z) = \sum_{j=1}^{n \cdot m} \sigma_j \cdot \iint_{S_j} \left(\frac{1}{r_j} + \frac{1}{r'_j} \right) ds \quad (5)$$

where σ_j is the strength of Rankine source, $1/r_j = 1/\sqrt{(x-x_j)^2 + (y-y_j)^2 + (z-z_j)^2}$ denotes unit strength of Rankine source, $1/r'_j = 1/\sqrt{(x-x_j)^2 + (y-y_j)^2 + (z+z_j+2H)^2}$ is the mirror image of $1/r_j$ about the water bottom, (x, y, z) and (x_j, y_j, z_j) is the field point and source point, respectively.

The bottom boundary condition are satisfied automatically for using the mirror image method. Combining Eq. (3) and Eq. (5), Laplace's equation can be solved numerically. The $m \cdot n$ unknowns are σ_j , evaluated at the panel center. Here the bi-Laplacian ∇^4 is discretized by centered finite differences in the x - and y -directions with 13 points, and the derivatives in the x -direction are calculated by using 3 point upstream finite differences. The integral along the x -axis are calculated by the trapezoidal rule. In particular, the integral in formula (5) and its partial derivative in the z -direction are calculated by Hess-Smith method [4].

After getting the values of source densities σ_j we can solve the disturbance potential φ by Eq. (5), and the vertical deformation η of the interface and wave resistance R acting on the load can be calculated by

$$\eta(x, y) = \frac{1}{U} \int_x^{+\infty} \frac{\partial \varphi}{\partial z} dx \quad (6)$$

$$R = \iint_{\Omega} P \frac{\partial \eta}{\partial x} dx dy \quad (7)$$

where Ω is the area of load distribution. The dimensionless wave resistance coefficient is $C_w = 2R\rho_w g / LP_0^2$.

3. Results and discussion

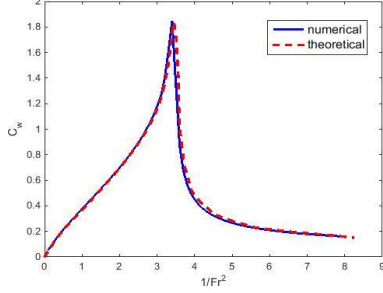


Fig. 2 Wave resistance

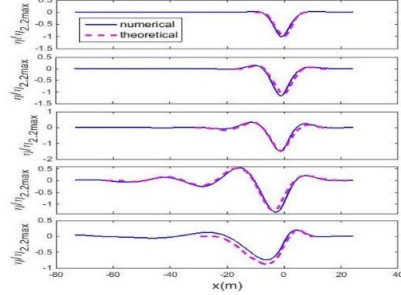
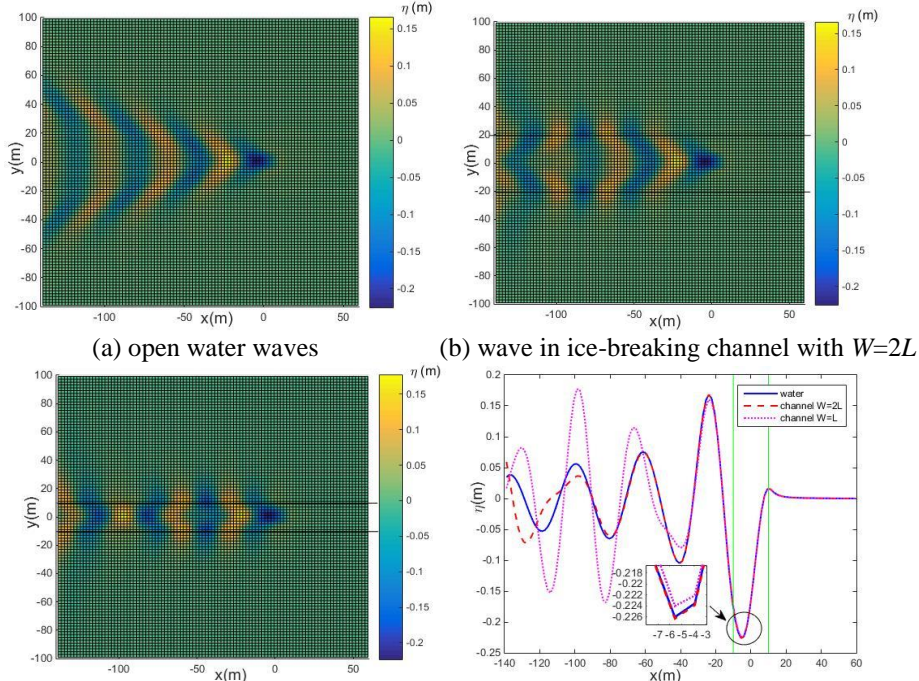


Fig. 3 Wave profile

Before studying the response of the moving load in ice-breaking channel, we firstly validate our procedure by comparing the results on the ice sheet with the theoretical solutions. On the one hand, wave resistance is concerned. The theoretical solutions come from [5], where $L/B=2$, $h=0.2$ m, $H=6$ m, $L=20$ m, $G=2$ GPa and $\tau=1$ s. Here we simulate the cases with same parameters. The results in Fig. 2 show the resistance coefficients under different speed or Froude number $Fr = U / \sqrt{gL}$. It can be seen that numerical results agree quite well with the theoretical results.

On the other hand, the deflection of the ice sheet or the induced wave is also concerned. The theoretical solutions come from [3], where $L/B=2.56$, $h=0.075$ m, $H=6.8$ m, $L=1.23$ m, $P_0=406.5$ Pa, $G=1.875$ GPa and τ given by formulas (3.1) in reference [3]. Here we simulate the cases with same parameters. Fig. 3 gives the vertical displacement of the ice sheet at a distance $y=1$ m away from the central line of the moving load. The different speed curves, from top to bottom, are 2.2m/s, 4.2m/s, 5.5m/s, 6.2m/s, 8.9m/s, respectively. Each displacement η at different speed is normalized through $\eta / \eta_{2.2max}$, where the denominator is the maximum displacement at 2.2m/s and is believed to be the maximum static displacement approximately. We can find that the numerical results are in qualitative agreement with the theoretical results, although there are still small differences between them. The differences may be caused by the truncated boundaries mainly in numerical simulation. Nevertheless, it is reasonable to believe that the method and procedure are valid to calculate this problem.



(a) open water waves (b) wave in ice-breaking channel with $W=2L$ (c) wave in ice-breaking channel with $W=L$ (d) wave profile at central line of the load, where the range between two vertical line is the span of pressure
Fig. 4 Wave produced by the load moving in ice-breaking channel with $Fr = 0.54$.

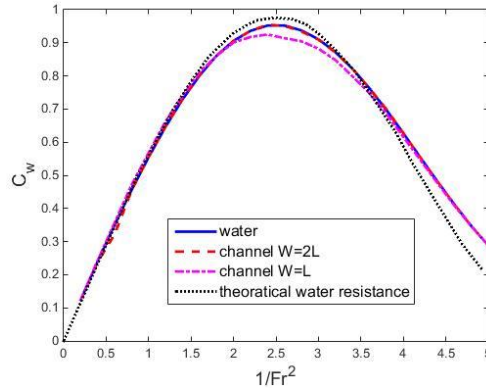


Fig. 5 Comparison of wave resistance coefficient for the load moving in water and ice-breaking channel with different width.

The calculation parameters are given as $L/B=2$, $h=0.2$ m, $L=20$ m, $P_0=1000$ Pa, $E=1.875$ GPa, $\tau=1$ s and infinite water depth. Fig. 4 shows the wave induced by the moving pressure moving in the ice-breaking channel and Fig.5 provides the wave resistance along with moving velocity accordingly. It should be noted that the Kelvin wave generated in the open water, as shown in Fig.4 (a), is no longer formed behind the load. The wave behind the load will be restricted in the channel and an inverted V-shaped wave will be formed, as presented in Fig. 4(b) and Fig. 4(c). On the other hand, from the wave curve of the center profile in Fig. 4(d), we can see that the wave profile in a wider channel closes to that in the open water more while the wave in a narrower channel present a much different pattern, as one can image. However, it is interesting to notice that all three cases have very similar wave profiles in the region right below the load in Fig. 4(d) and their wave resistances close to each other in Fig. 5. From Eq. (7), wave resistance only relies on the wave profiles in the region right below the load, so it can be understood that similar profile under the load induces similar resistance. As the channel becomes narrower, the abrupt change of boundary condition at $|y|=W/2$ influences more and affects the wave resistance especially in medium speed. Lastly, the difference between calculated and theoretical results in the resistance curve in open water may be mainly caused by the accuracy of the grids.

4. Conclusions

The paper studies the wave pattern and resistance of a pressure load moving in the ice-breaking channel by boundary element method. It is found that the wave behind the load will be restricted in the channel and an inverted V-shaped wave will be generated. However, the wave profile right below the load will not change much with different width of ice-breaking channel, which leads to similar wave resistance as long as the channel is wider than the load.

Acknowledgment

This work is supported by the National Key R&D Program of China (No. 2017YFE0111400), National Natural Science Foundation of China (Nos. 51639004 and 51579054), the Fundamental Research Funds for the Central Universities (No. HEUCFG201811), to which the authors are most grateful.

Reference

- [1] Squire V A, Hosking R J, Kerr A D, et al. Moving Loads on Ice Plates[M]. Springer Netherlands, 1996.
- [2] Li Y, Liu J, Hu M, et al. Numerical modeling of ice-water system response based on Rankine source method and finite difference method[J]. Ocean Engineering, 2017, 138:1-8.
- [3] Kozin V M, Pogorelova A V. Effect of the viscosity properties of ICE on the deflection of an ICE sheet subjected to a moving load[J]. Journal of Applied Mechanics & Technical Physics, 2009, 50(3):484-492.
- [4] Dai Y.S, Duan W.Y. Potential flow theory of ship motion in waves[M]. National Defence Industry Press, 2008.
- [5] Kozin V M, Pogorelova A V. Wave Resistance of Amphibian Aircushion Vehicles During Motion on Ice Fields[J]. Journal of Applied Mechanics & Technical Physics, 2003, 44(2):193-197.